

Alloying effects on the microstructure and phase stability of Fe–Cr–Mn steels

James C. Rawers

Received: 22 November 2006 / Accepted: 26 February 2008 / Published online: 23 March 2008
© Springer Science+Business Media, LLC 2008

Abstract Austenitic Fe–Cr–Mn stainless steels interstitially alloyed with nitrogen have received considerable interest lately, due to their many property improvements over conventional Fe–Cr–Ni alloys. The addition of nitrogen to Fe–Cr–Mn stabilizes the fcc structure and increases the carbon solubility. The benefits of increased interstitial nitrogen and carbon content include: enhanced strength, hardness, and wear resistance. This study examines the effect of carbon, silicon, molybdenum, and nickel additions on the phase stability and tensile behavior of nitrogen-containing Fe–Cr–Mn alloys. Nitrogen and carbon concentrations exceeding 2.0 wt.% were added to the base Fe–18Cr–18Mn composition without the formation of nitride or carbide precipitates. Minor additions of molybdenum, silicon, and nickel did not affect nitrogen interstitial solubility, but did reduce carbon solubility resulting in the formation of $M_{23}C_6$ (M=Cr, Fe, Mo) carbides. Increasing the interstitial content increases the lattice distortion strain, which is directly correlated with an increase in yield stress.

Introduction

Iron–chromium–manganese steels are not only less expensive than comparable iron–chromium–nickel stainless steels but can be designed to have higher strength, wear and creep resistance [1–5]. The strength of Fe–Cr–Mn steels can be increased more than three-fold by alloying

with nitrogen [2, 4, 6–8]. The substitution of manganese for nickel enhances the alloy's nitrogen interstitial solubility. Recently, high-nitrogen Fe–Cr–Mn–N steel alloys have been shown to also have an enhanced solubility for carbon [9–17]. Carbon also enters the alloy as an interstitial. Thus these Fe–Cr–Mn–N–C alloys have increased the total interstitial concentration resulting in further increasing the alloy strength [2, 4, 5, 8, 9, 12, 13]. Two atomic phenomena have been observed that help explain the enhanced carbon–nitrogen interstitial concentration and the resulting effect on material properties [14, 16, 17]. The first has resulted from electron-spin-resonance experiments in which the free electron concentration of alloys for the combination of nitrogen and carbon is greater than the sum of the individual components [14, 16, 17]. The higher free electron concentration promotes the metallic structure and stable fcc phase, and suppresses the formation of precipitates. The second has resulted from Mossbauer experiments that have shown the presence of one interstitial nearest neighbor only, no next nearest neighbor neighbors [14, 16, 17]. Neither carbon nor nitrogen occupies adjacent interstitial sites within the first and second coordination spheres [16]. This promotes interstitial solubility and reduces the chance of precipitate formation.

The interstitial stability of high levels of nitrogen and carbon in iron-based alloys was first discovered and characterized in alloys systems that contained only iron, nitrogen, and carbon [14, 16, 18, 19]. In these studies, the high concentrations of nitrogen were introduced into ferritic Fe–C alloys that resulted in the formation of stable, solid-solution, single-phase, precipitation-free, high interstitial, austenitic Fe–N–C alloys. These Fe–N–C alloys were investigated to determine if it might be possible to extend the temperature range of the fcc phase by alloying with nitrogen and carbon. The fcc to bcc phase transition

J. C. Rawers (✉)
National Energy Technology Laboratory, U.S. Department
of Energy, Albany, OR, USA
e-mail: James.Rawers@NETL.DOE.GOV

for pure iron occurs at 911 °C, for Fe–C at 723 °C, and for Fe–N at 590 °C. In the fcc phase both Fe–C and Fe–N have a solid-solution range approaching 2 wt.% at elevated temperatures. Moreover, in Hadfield's steels, carbon levels in excess of 1.0 wt.% remain in solution and are necessary to ensure the alloy remain fcc down to room temperature in these Fe–Mn–C compositions [20].

In stainless steel alloys, interstitial concentration can be increased by varying the base composition (manganese increases nitrogen solubility, nickel decreases nitrogen solubility [1, 3]). Fe–18Cr–18Mn stainless steel alloys melted at atmospheric pressure have a nitrogen concentration limitation of 0.4–0.6 wt.% [20]. It is interesting to note here that above approximately 0.5 wt.% the free electron concentration begins to decrease [16]. The interstitial nitrogen concentration can also be increased by increasing the nitrogen gas pressure over the molten liquid during melting. Nitrogen solubility followed Sievert's Law, nitrogen in the melt is proportional to the $\sqrt{(\text{nitrogen gas pressure over the melt})}$ [1, 3]. Carbon has limited solubility in stainless steels, and readily forms carbides, preferentially with chromium. Thus, carbon is thus not generally added to Fe–Cr–Ni stainless steels [2, 9, 14]. Similarly,

nitrogen also has limited solubility in Fe–Cr–Ni stainless steels resulting in the formation of nitrides.

Silicon and molybdenum are commonly added to steels to enhance oxidation and corrosion resistance. Nickel is alloyed to improve machinability [1, 12]. Alloying with silicon and molybdenum is predicted to reduce the interstitial solubility, and thus enhance the chance of precipitate formation [1]. The object of this study was to characterize and evaluate the phase stability and microstructure of Fe–Cr–Mn–N steels alloyed with carbon and with minor, solid-solution additions of nickel, molybdenum, and silicon.

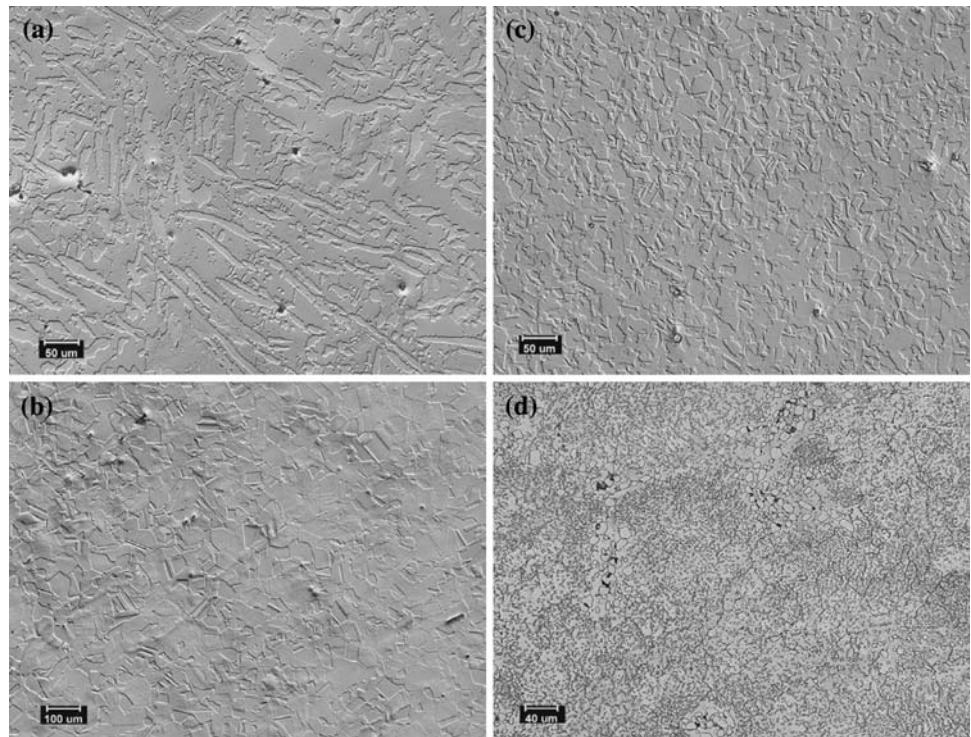
Experimental procedure

Twenty-five 1 kg mixtures of 99.9% pure elemental compacted particles were melted in an environmentally controlled induction furnace. Melt atmosphere was either pure argon (Alloys D1 thru D5) or pure nitrogen (all other alloys). Nitrogen melt pressures are listed in Table 1. Ingots were then homogenized at 1,150 °C for 12 h in a vacuum furnace. Alloys were forged and hot rolled at 1,150 °C using 25–30% reductions to a final thickness of

Table 1 Alloy table: alloy chemistry (wt.%), d-spacing (nm), yield (MPa), melt nitrogen pressure (MPa)

	Fe	Cr	Mn	Ni	Mo	Si	N	C	d-space	Phases	Yield	Melt
D1	69.5	14.9	14.6	0.0	0.0	0.0	0.01	0.03	0.3595	fcc–bcc	269	0.0
D2	64.4	17.9	17.7	0.0	0.0	0.0	0.00	0.01	0.3594	fcc–bcc	339	0.0
D3	63.9	14.3	21.3	0.0	0.0	0.0	0.01	0.02	0.3597	fcc–bcc	497	0.0
D4	62.4	15.2	22.0	0.0	0.0	0.0	0.01	0.02	0.3603	fcc–bcc	528	0.0
D5	58.3	16.4	24.5	0.0	0.0	0.0	0.01	0.01	0.3607	fcc–bcc	594	0.0
F1	60.4	14.8	24.1	0.0	0.0	0.0	0.29	0.01	0.3619	fcc	258	0.05
F2	64.4	17.9	17.1	0.0	0.0	0.0	0.56	0.03	0.3618	fcc	300	0.1
F3	63.7	15.0	20.3	0.0	0.0	0.0	0.61	0.01	0.3624	fcc	372	0.1
F4	68.2	14.6	16.5	0.0	0.0	0.0	0.22	0.52	0.3621	fcc	629	0.05
F5	62.1	14.7	22.0	0.0	0.0	0.0	0.50	0.31	0.3629	fcc	442	0.1
F6	62.7	15.0	21.1	0.0	0.0	0.0	0.43	0.35	0.3627	fcc	386	0.1
F7	63.4	17.5	18.2	0.0	0.0	0.0	0.43	0.46	0.3622	fcc	598	0.1
F8	69.1	14.2	14.8	0.0	0.0	0.0	0.94	0.36	0.3621	fcc	560	1.0
F9	70.0	13.8	14.2	0.0	0.0	0.0	0.88	0.46	0.3623	fcc	598	1.0
F10	71.0	13.7	12.0	0.0	0.0	0.0	1.67	0.41	0.3629	fcc	872	4.0
M1	62.7	16.1	17.8	1.9	0.91	0.34	0.58	0.04	0.3621	fcc	624	0.2
M2	60.9	16.5	18.7	1.9	1.10	0.30	0.60	0.03	0.3624	fcc	724	0.2
M3	65.1	16.0	11.7	0.4	1.04	0.51	0.71	0.03	0.3628	fcc	747	0.4
M4	60.6	17.4	12.5	1.0	0.99	0.43	0.89	0.11	0.3630	fcc	764	0.6
P1	61.1	17.4	17.6	1.8	0.87	0.34	0.52	0.44	0.3622	fcc, M ₂₃ C ₆	668	0.2
P2	61.9	16.2	17.6	1.9	0.75	0.38	0.53	0.64	0.3622	fcc, M ₂₃ C ₆	680	0.2
P3	65.4	15.3	15.1	0.0	2.20	0.87	0.76	0.49	0.3624	fcc, M ₂₃ C ₆	710	1.0
P4	60.6	17.0	17.9	1.9	0.86	0.25	0.45	0.91	0.3622	fcc, M ₂₃ C ₆	722	0.2

Fig. 1 (a) Base alloy: duplex-phase microstructure: fcc and bcc Fe–18Cr–18Mn (Alloy D1) (b) Base alloy plus both interstitial nitrogen and carbon interstitials: fcc-phase only Fe–18Cr–18Mn–0.43N–0.46C (Alloy F7) (c) Base Alloy plus Ni, Mo, and Si minor solutes and interstitial nitrogen: fcc-phase only Fe–16Cr–12Mn–0.4Ni–1.0Mo–0.51Si–0.70N–0.03C (Alloy M3) (d) Base Alloy plus minor solutes and both nitrogen and carbon interstitials: fcc-phase with $M_{23}C_6$ precipitates uniformly distributed throughout the microstructure Fe–19Cr–18Mn–1.9Ni–0.3Mo–0.40Si–0.63N–0.64C (Alloy P4)



3 mm. After hot working, the alloys were heat treated at 1,150 °C for 30 min and air-cooled. Samples were then sectioned: (i) for chemical analysis (Table 1), (ii) for optical microscopy, and (iii) for X-ray diffraction analysis. Chemical analysis for nitrogen and carbon was conducted on LECO gas analyzers. Metallic component concentrations were determined both by X-ray fluorescence and induction coupled plasma. Microstructure was determined using high-resolution optical micrographs (Fig. 1a–d). Phase identification and lattice fcc-[100] d-spacing were obtained from X-ray diffractographs (Table 1). Samples were also machined for sheet tensile tests and tested at room temperature in accordance with ASTM E-8.

Results

The observed alloy phases are consistent with compositional calculations and predictions of the Schaeffler diagram (Fig. 2) [21]. Chemical analysis, fcc [100] lattice d-spacing, and tensile yield stress for the alloys are listed in Table 1. The alloys are divided into four categories: (1) Fe–Cr–Mn alloys with a duplex fcc–bcc phase microstructure, (2) Fe–Cr–Mn–N–C alloys with a single-phase microstructure, (3) Fe–Cr–Mn–N alloys with minor solid-solute additions of molybdenum, silicon, and nickel with a single-phase microstructure, and (4) Fe–Cr–Mn–(Mo–Si–Ni)–N–C alloys with fine carbide precipitate uniformly distributed through the fcc phase. Within each category, the

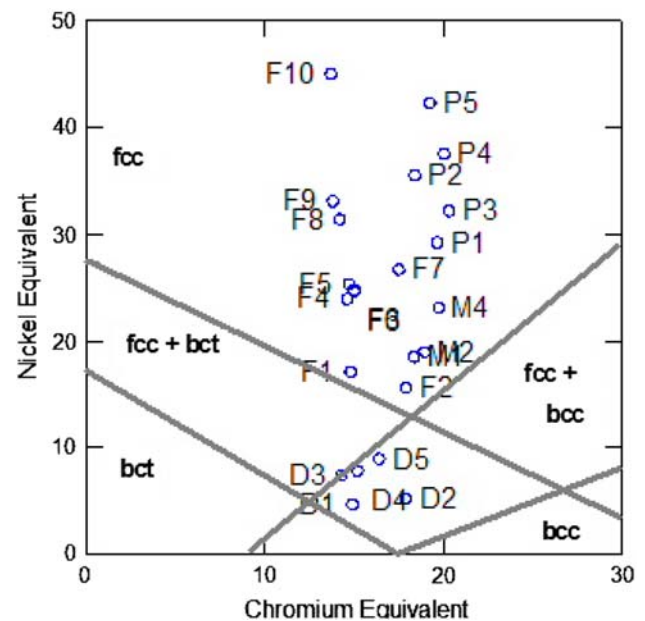


Fig. 2 Schaeffler diagram: alloy concentrations for Table 1 are plotted using the following equations [1]: Ni equivalent = Ni + (0.87 · Mn) + (30 · C) + (18 · N), Cr equivalent = Cr + Mo + (1.5 · Si)

alloys are ordered with respect to increasing total nitrogen and carbon concentration.

Predicted nitrogen concentrations were calculated combining Sievert's Law with respect to nitrogen pressure, $p(N_2)$, and alloy component chemistries' thermodynamic interaction equivalent factors, C_i , [1]:

$$[\%N]_{\text{calc}} = 0.0396 \cdot \sqrt{(p(N_2)/f_N)} \tag{1}$$

where f_N = activity coefficient of element i: $\log_{10}(f_N) = \sum e_N^{X_i} [\%X_i]$, $e_N^{X_i}$ = interaction parameter, X_i = element i concentration.

The measured nitrogen chemistries are consistent with those predicted for the alloy chemistries and melt pressures. Statistical analysis showed an R^2 value of 0.993 for a linear fit between the measured nitrogen concentration (Table 1) and calculated nitrogen concentrations.

[Note, the elemental concentrations in this manuscript are reported in weight percent, wt.%. This nomenclature is routinely used in designation of iron-based alloy compositions. To a first approximation, to convert to atomic percent: (i) for the major elements: iron, chromium, manganese (and nickel), the atomic percent approximately equals weight percent, and (ii) for the minor elements their contribution is small and to convert the interstitial nitrogen and carbon concentrations from weight percent to atomic percent multiply by 4, silicon multiply by 2, molybdenum divide by 2.]

Base alloy compositions, Alloys D1 thru D5: Fe–(15–18)Cr–(15–25)Mn.

The Fe–Cr–Mn base alloy composition has a duplex-phase microstructure: fcc (austenite) and bcc (ferrite) (Fig. 1a). X-ray diffractograph patterns show only fcc and bcc phases present. High-resolution optical microscopy did not show any evidence of bct phase (martensite). Increasing manganese concentration expands the fcc lattice and increases the yield strength.

Base alloy composition plus nitrogen and carbon, Alloys F1 thru F10: Fe–(14–18)Cr–(12–24)Mn–(0.01–1.67)N–(0.03–0.46)C.

The microstructure for the Fe–Cr–Mn base compositions alloyed with both (i) nitrogen, and (ii) nitrogen and carbon is single-phase fcc (Fig. 1b). The entire nitrogen and carbon concentration remains interstitial. There was no evidence of the formation of nitrides and carbides, even when the total nitrogen and carbon interstitial concentrations exceed 2 wt.%. Increasing the interstitial concentration expands the fcc lattice and increases yield strength.

Base alloy compositions plus nitrogen and Si, and Mo additions, Alloys M1 thru M4: Fe–(12–16)Cr–(12–19)Mn–(0.4–2.0)Ni–(0.2–1.0)Mo–(0.4–1.0)Si–(0.6–0.9)N.

The microstructure for the base alloy with nitrogen and with minor solid-solute elements: molybdenum, silicon, or nickel additions, is single-phase fcc (Fig. 1c). X-ray diffraction confirms only the fcc phase was present. Increasing the interstitial content expands the fcc lattice by increasing the yield strength.

Base alloy composition plus nitrogen and carbon and Si, Mo, and Ni addition minor solutes, Alloys P1 thru P5:

Fe–(15–19)Cr–(15–18)Mn–(0–1.9)Ni–(0.3–2.2)Mo–(0.4–0.9)Si–(0.4–0.8)N–(0.4–0.9)C.

The matrix microstructure is single-phase fcc with a uniform dispersion of 10–20 micron precipitates (Fig. 1d). X-ray diffraction analysis shows the precipitate to be $M_{23}C_6$. These alloys were further investigated using SEM-Energy Dispersive Spectroscopy. Precipitates had an average metallic chemistry of 50-Cr, 17-Mn, 29-Fe, 2.8-Mo, and 0.55-Ni, with no silicon. (The precipitate size was such that the SEM beam probably extended into the metal matrix.) For these alloys with precipitates, there is a direct correlation between the lattice d-spacing and the yield strength.

Discussion

The Schaeffler diagram is a well-documented means of predicting phase composition of designing stainless steel alloys. For a given alloy chemistry, determination of the different matrix phases: fcc, bcc, and bct, and the approximate proportion of each phase is predicted in terms of nickel and chromium weight percent equivalents [1, 19]:

$$\text{Ni equivalent} = \text{Ni} + (0.87 \cdot \text{Mn}) + (30 \cdot \text{C}) + (18 \cdot \text{N}) + \dots \tag{2a}$$

$$\text{Cr equivalent} = \text{Cr} + \text{Mo} + (1.5 \cdot \text{Si}) + \dots \tag{2b}$$

A plot of the alloy chemistries onto the Schaeffler diagram successfully predicted the observed phases. The role of interstitial nitrogen and carbon in stabilizing the fcc phase is well documented [2, 3, 5, 9, 14]. However, the Schaeffler formulation cannot be used to predict when, or if, precipitates (such as nitride and/or carbide) will form.

A recent study [22] supports the finding in this study that the base alloy chemistry, Fe–18Cr–18Mn, has a duplex microstructure (bcc–fcc) until the nitrogen concentration exceeds approximately 0.3 wt.%, after which, with increasing the nitrogen concentration, the alloy remains fcc. Previous stainless steel studies have shown that silicon slightly decreased nitrogen solubility; molybdenum significantly increased nitrogen solubility [1]. However, nitrogen concentrations approaching 0.90 wt.% remained interstitial in these alloys, even with minor additions of Si, Mo, or Ni.

This study shows that when in combination with nitrogen concentrations from 0.3 to 1.5 wt.%, carbon concentrations between 0.0 and 0.5 wt.% remain interstitial in Fe–Cr–Mn alloys. However, when carbon was added to alloys containing the minor alloy additions of silicon and molybdenum, $M_{23}C_6$ precipitates formed. $M_{23}C_6$ precipitates form in these alloys as a result of the combined effects of silicon, reported to reduce interstitial solubility, and

molybdenum, known to enhance formation of precipitates [1, 21, 23–29].

The fcc-phase lattice dimension is a function of the alloy composition: (i) the lattice expands when the larger radius atoms of elements such as molybdenum, manganese, or silicon [1] are substituted into the fcc lattice for iron and chromium atoms, and/or (ii) the lattice expands when nitrogen and carbon are placed interstitially into the fcc octahedral void sites [30]. The solid-solution radius of iron, chromium, and nickel atoms is approximately 0.125 nm, and that of manganese, silicon, and molybdenum is approximately 0.135 nm [20]. In the fcc lattice, interstitial C and N fit into the octahedral void site, expanding the 0.05 nm void to accommodate the 0.07 nm radius of the carbon and nitrogen interstitial atoms [1]. Both these lattice expansion effects were observed. Preliminary results between the lattice expansion and alloy strength are presented. (An in-depth analysis of strength microstructure can be found in Ref. [31].)

For the interstitial free alloys, the change in the fcc (100) lattice dimension of the base alloy compositions was determined to be directly related to the manganese concentration:

$$\begin{aligned} \text{fcc (100) lattice d-spacing (nm)} \\ = 0.3594 + 0.00012 \cdot [\text{Mn, wt.\%}]. \end{aligned} \quad (3a)$$

The expanded lattice and resulting internal stress increased the yield strength linearly with increasing manganese concentration:

$$\text{yield (MPa)} = 250 + 34 \cdot [\text{Mn, wt.\%}]. \quad (3b)$$

In the solid solution, interstitial alloys, the fcc lattice expansion was also directly proportional to the interstitial concentration. The strengthening contributions for either nitrogen or carbon were determined to be similar (within one standard deviation) and thus can be combined. The combined effect of the manganese solid solution and nitrogen plus carbon interstitial lattice expansion is:

$$\begin{aligned} \text{fcc (100) d-spacing (nm)} = 0.3592 + 0.00011 \cdot [\text{Mn, wt.\%}] \\ + 0.0012 \cdot [\text{N} + \text{C, wt.\%}]. \end{aligned} \quad (4a)$$

The lattice d-spacing and the increase in alloy strength are approximately a factor of ten greater for interstitials than the matrix solid-solution contribution. A similar effect of interstitial versus solid-solution concentration can be found on their effect on yield strength:

$$\begin{aligned} \text{Yield (MPa)} = 251 + 33 \cdot [\text{Mn, wt.\%}] + 313 \cdot [\text{N} \\ + \text{C, wt.\%}]. \end{aligned} \quad (4b)$$

The effect of alloy composition on the formation and quantity of precipitates was determined from the total concentration of nitrogen and carbon, the lattice expansion, and microscopy. Optical microscopy shows a uniform distribution of precipitates. X-ray diffraction indicated these precipitates to be $M_{23}C_6$. The fcc lattice dimension for the alloys increased linearly with increasing nitrogen and carbon concentration. Alloys with precipitates all had similar lattice displacement, suggesting the interstitial concentration in these alloys was similar. (The increase in lattice dimension for P3 is due to the enhanced concentration of larger solute atoms, silicon and molybdenum.) The expanded lattice dimensions suggest an interstitial concentration of approximately 0.62 wt.% nitrogen and carbon. Because the precipitates were only carbides, the difference in the total nitrogen and carbon concentration and the interstitial concentration is the loss of interstitial carbon that is now carbide precipitates. The percent carbides predicted and that measured using optical microscopy image analysis are in close agreement (Table 2).

Assuming the carbide calculations to be accurate it is also possible to obtain an approximation as to the increase in strength due to precipitates. The change in yield strength for precipitates is approximately 100 MPa for each weight percent carbon in precipitates. This is in contrast to approximately 30 MPa for each weight percent solid-solution strengthening, and for over 300 MPa for each weight percent carbon interstitial (Eq. 4b).

Table 2 Carbide concentration determined from total nitrogen and carbon concentration and lattice expansion. Calculated and measured carbide concentration. And, yield strength enhancement due to precipitates

	(N + C) _{total} (wt.%)	(C) _{carbide} ^a (wt.%)	% of carbide calculated	% of carbide measured	σ_{yield} (MPa)	$\sigma_{\text{yield}} - \sigma_{\text{interstitial}}^b$
P1	0.96	0.34	7	6–7	668	28
P2	1.17	0.55	11	8–11	680	40
P3	1.25	0.63	13	10–14	710	70
P4	1.36	0.74	15	15–18	722	82

^a Measured total nitrogen and carbon concentration minus 0.62 wt.% interstitial as determined from alloy M1 interstitial concentration with similar lattice dimensions 0.3622 nm

^b Measured yield strength minus 640 MPa as determined from M1 for interstitial strength

In summary, Fe–18Cr–18Mn has a duplex, bcc–fcc microstructure. Lattice expands in direct proportion to the increase in the concentration of the larger atom size of the solid-solution manganese concentration. The increase in manganese produces an increase in solid-solution strengthening.

Fe–18Cr–18Mn–N has a solid-solution, fcc microstructure. Nitrogen goes into the alloy as an interstitial. Lattice expansion is directly proportional to interstitial nitrogen concentration. Yield strength increases in proportion to increasing interstitial concentration.

Fe–18Cr–18Mn–N–C has a solid-solution fcc, solid-solution microstructure. Both nitrogen and carbon go into the alloy as interstitials. Lattice expansion is directly proportional to the interstitial concentration, the total nitrogen and carbon concentration. Yield strength increases in proportion to the total interstitial concentration. Interstitial strengthening is approximately ten times more effective than solid solution strengthening.

Fe–18Cr–18Mn–(Si/Mo/Ni)–N has a solid-solution, fcc matrix phase. Silicon, molybdenum, and nickel addition went in as substitution lattice atoms and did not result in formation of nitride precipitates. Both interstitial and solid-solution strengthenings are observed.

Fe–18Cr–18Mn–(Si/Mo/Ni)–N–C has fcc matrix phase with finely dispersed $M_{23}C_6$ precipitates. From the measurement of lattice expansion, these alloys had a uniform interstitial concentration, regardless of the total added nitrogen and carbon concentration. Yield strength increased due to the interstitial concentration which was approximately solely due to the nitrogen concentration and in direct proportion to the carbide precipitate concentration. Yield strength, precipitation strengthening was only a third as effective as interstitial strengthening.

Conclusion

The phase evolution of Fe–Cr–Mn alloys is strongly affected by alloy chemistry. Fe–18Cr–18Mn alloy is fcc–bcc duplex phase. Nitrogen enters Fe–Cr–Mn alloys as an interstitial. Nitrogen not only stabilizes the fcc phase, but also increases carbon solubility. Minor alloy additions of molybdenum, silicon, and nickel do not affect nitrogen interstitial solubility, but do reduce carbon solubility resulting in formation of $M_{23}C_6$ precipitates. The addition of larger solute substituted atoms and interstitials increases the lattice dimensions. There is a direct correlation between lattice expansion and yield strength. Increasing the interstitial concentration increases the yield strength by approximately a factor of ten more than does solute substitution. Precipitates increase yield strength but only a factor of three more than solution strengthening.

References

- Gavriljuk V, Berns H (1999) High nitrogen steels. Springer-Verlag, ISBN 3-540-66411-4
- Berns H, Gavriljuk V (2007) Key Eng Mater 345–346:421
- Foet F (2003) High nitrogen steels and interstitial alloying. HNS 2003, Schaffhausen, Switzerland, 26–28 March 2003
- Rawers J (2004) Proc Instn Mech Eng vol 218, Part L, J Mater Des Appl, pp 239
- Rawers J, Tylczak J (2003) Characterizing alloy additions to high-nitrogen steels. THERMEC 2003, Leganes, Madrid, Spain, 7–11 July 2003
- Menzel J, Stein G (1988) Dahlmann P Massive nitrogen-alloyed austenitic bolt materials. HNS 1988, Lille, France, 18–20 May 1988
- Uggowitzer P, Harzenmoser M (1988) Strengthening of austenitic stainless steels by nitrogen, HNS 1988, Lille, France, 18–20 May 1988
- Speidel M (1990) Properties of high nitrogen steels. HNS 1990, Aachen Germany, 10–12 Oct 1990
- Rawers J (2003) Preliminary study into the stability of interstitial nitrogen and carbon in steels. HNS 2003, Schaffhausen, Switzerland, 26–28 March 2003
- Berns H (2003) Alloy development and processing. HNS 2003, Schaffhausen, Switzerland, 26–28 March 2003
- Speidel M (2003) From high-nitrogen steels to high interstitial alloys. HNS 2003, Schaffhausen, Switzerland, 26–28 March 2003
- Bernauer J, Gabriele S, Speidel M (2004) Combined influence of carbon and nitrogen on the mechanical and corrosion properties of Cr–Mn steel grade, HNS 2004, Ostend, Belgium, 19–22 Sept. 2004
- Schmalt F, Berns B, Gavriljuk V (2004) Mechanical Properties of a stainless austenitic CrMnCN steel, HNS 2004, Ostend, Belgium, 19–22 Sept. 2004
- Gavriljuk V, Rawers J, Shanina B, Berns H (2003) Mater Sci Forum 426–432:943
- Dong H, Lin Q, Rong F, Su J, Xin C, Lang Y, Kang X (2003) Development and applications of nitrogen alloyed stainless steels in China. HNS 2003, Schaffhausen, Switzerland, 26–28 March 2003
- Gavriljuk V, Shanina B, Berns H, Mater Sci Eng A (in press)
- Shanina B, Gavriljuk V, Berns H (2007) Mater Sci Forum 539–543:4993
- Rawers J, Uggowitzer P (1998) Characterization of Fe–C/N steel. HNS 1998, Espoo, Finland, 24–29 May 1998
- Rawers J (2003) WEAR 258:32
- METALS Desk Handbook (1985) chpt. 15, ASM, pp 30, ISBN: 0-87170-188-X
- Gersten J, Smith F (2001) The physics and chemistry of materials. J. Wiley and Sons, p 63, ISBN 0-471-05794-0
- Liang J, Yang Z, Li W, Yi B (2006) Study of the properties of high-nitrogen stainless steel in 1Cr18Mn18N. HNS conference, Jiuzhaigong, Siuhaun, China, 29–30 Aug 2006
- Kikuchi K, Kajihari M, Frisk K (1988) Solubility of nitrogen in austenitic stainless steel. pp 63, HNS 1988, Lille, France, 18–20 May 1988
- Kim S, Lee T (1998) Precipitation sequence in austenitic steels. pp 109, HNS1998, Lille, France, 18–20 May 1988
- Wahlberg G, Rolander G, Andren H (1998) Interaction between nitrogen and substitutional elements in austenitic stainless steels. pp 163, HNS 1998
- Anthanahen B, Uggowitzer P, Cui M, Speidel M, Stein G (1998) New high nitrogen ferritic steels. pp 58, HNS 1998
- Foet F, Magnii T, Perrot P, Vogt J (1991) Duplex stainless steel '91. Bougogne, France, pp 49, 28–30 Oct 1991

28. Guttman M (1991) In: Gunn RN (ed) Duplex stainless steels. William Andrew Plb, p 79, ISBN 9781884207617
29. Bavay J (1993) In: Lacombe P, Baroux B, Beranger B (eds) Stainless steels. Les Editions de Physique, Les Ulis, Cedex A, France, p 551, ISBN 2-86883-189-3
30. Cheng L, Bottger A, deKeijser T, Mittemeijer E (1990) Scripta Metall Mater 24:509
31. Rawers J, Dutlinger N, Mater Sci Technol (accepted for publication)